Inorg. Chem. **2006**, *45*, 1945–1950

The First Metal-Based Paullone Derivative with High Antiproliferative Activity in Vitro

Anatoly Dobrov,[†] Vladimir B. Arion,*[,†] Norbert Kandler,[†] Werner Ginzinger,[†] Michael A. Jakupec,[†] Anna Rufińska,[‡] Nikolai Graf von Keyserlingk,[§] Markus Galanski,[†] Christian Kowol,[†] and Bernhard K. Keppler*[,†]

Institute of Inorganic Chemistry, University of Vienna, Waehringerstrasse 42, A-1090 Vienna, Austria, Max-Planck-Institut für Kohlenforschung, Kaiser-Wilhelm-Platz 1, D-45470 Mülheim an der Ruhr, Germany, and Faustus Forschungs Compagnie, Translational Cancer Research GmbH, Grimmaische Strasse 2-4, D-04109 Leipzig, Germany

Received July 5, 2005

9-Bromo-7,12-dihydroindolo[3,2-*d*][1]benzazepin-6(5*H*)-one, kenpaullone, which displays similarities in the activity profile to flavopiridol, was modified by chemical transformations at the lactam unit to provide a peripheral binding site able to accommodate metal ions. The first metal-based paullone has been prepared and characterized by single-crystal X-ray diffraction methods, solid-state cross-polarization magic angle spinning ^{13}C NMR spectroscopy, electrospray ionization mass spectra, and electronic spectra. The gallium complex $[GaL_2]Cl\cdot 2.5H_2O$, the metal-free ligand (HL), and the starting compound used for the preparation of HL were assessed in vitro for their cytotoxicity in a panel of human tumor cell lines. The gallium complex was found to be 1.5–18-fold more cytotoxic than HL, with an average IC_{50} value of 2.0 μM.

Introduction

Analysis of the National Cancer Institute (NCI) Human Tumor Cell Line Anti-Cancer Drug Screen Database showed that 9-bromo-7,12-dihydroindolo[3,2-*d*][1]benzazepin-6(5*H*)-one[1] (**1**, kenpaullone; see Chart 1) exhibits a similar activity profile to flavopiridol, a well-known inhibitor of cyclin-dependent kinases (CDKs).[2,3] Subsequent investigations with enzyme assays proved kenpaullone to inhibit CDK1/cyclin B, CDK2/cyclin A, and CDK5/p25, though less efficiently than flavopiridol. The search for more potent paullone-related CDK inhibitors with improved antitumor activity revealed that the substitution of bromine in position 9 by other more electron-withdrawing groups such as cyano or especially a nitro group enhances the kinase-inhibiting potency. Favorable effects were also exerted by methoxy groups or aminoalkyl side chains in position 2 or 3, while substitutions at the nitrogen atoms (positions 5 and 12) and at the methylene group (position 7), as well as replacement of the lactam unit by a thiolactam, a thioimidate, or a hydroxyamidine, resulted in decreased CDK inhibition.[4] At the same time, the antiproliferative activity of the prepared derivatives is not necessarily paralleling the CDK inhibitory profile.[4,5]

Chart 1. Kenpaullone, **1**

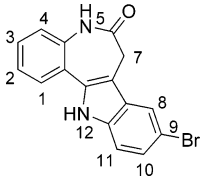

In particular, the N12-Boc-protected kenpaullone and the thioimidate **2** (Scheme 1) displayed remarkable antiprolif-

* To whom correspondence should be addressed. E-mail: vladimir.arion@univie.ac.at (V.B.A.), bernhard.keppler@univie.ac.at (B.K.K.). Fax: +43 1 4277 52630 (V.B.A.), +43 1 4277 52680 (B.K.K.).
† University of Vienna.
‡ Max-Planck-Institut für Kohlenforschung.
§ Faustus Forschungs Compagnie.

(1) Kunick, C. *Arch. Pharm. (Weinheim)* **1992**, *325*, 297−299.
(2) Zaharewitz, D. W.; Gussio, R.; Leost, M.; Senderowitz, A. M.; Lahusen, T.; Kunick, C.; Meijer, L.; Sausville, E. A. *Cancer Res.* **1999**, *59*, 2566−2569.
(3) Sausville, E. A.; Zaharewitz, D.; Gussio, R.; Meijer, L.; Louarn-Leost, M.; Kunick, C.; Schultz, R.; Lahusen, T.; Headlee, D.; Stinson, S.; Arbuck, S. G.; Senderowicz, A. *Pharmacol. Ther.* **1999**, *82*, 285−292.
(4) Schultz, C.; Link, A.; Leost, M.; Zaharevitz, D. W.; Gussio, R.; Sausville, E. A.; Meijer, L.; Kunick, C. *J. Med. Chem.* **1999**, *42*, 2909−2919.
(5) Wieking, K.; Knockaert, M.; Leost, M.; Zaharewitz, D. W.; Meijer, L.; Kunick, C. *Arch. Pharm. Pharm. Med. Chem.* **2002**, *7*, 311−317.

10.1021/ic0511120 CCC: $33.50
Published on Web 02/10/2006

Scheme 1. Reaction Pathways to **4** and **5**[a]

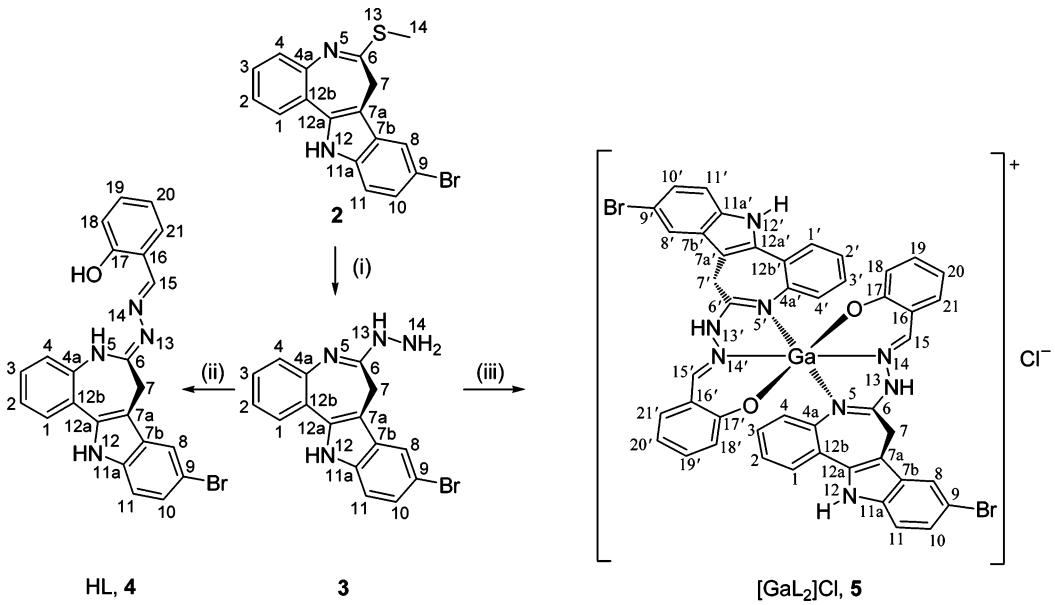

[a] Reagents and conditions: (i) $N_2H_4 \cdot H_2O$, C_2H_5OH, RT, 48 h (36%); (ii) 2-hydroxybenzaldehyde, CH_3OH, 68 °C, 40 min (93%); (iii) 2-hydroxybenzaldehyde, $GaCl_3$, CH_3OH, NEt_3, 68 °C, 35 min (55%). Complex **5** precipitates as $[GaL_2]Cl \cdot 2.5H_2O$.

erative activity in vitro, while being poor CDK1 inhibitors. This fact suggests additional intracellular targets besides CDKs for this class of compounds.[5−7] Chromatographic studies with paullone derivatives immobilized on an agarose matrix through an aminoalkyl linker in position 2 or 3 showed these compounds to possess affinity to the glycogen−synthase kinase-3α (GSK-3α) and GSK-3β as well as mitochondrial malate dehydrogenase.[8] In addition, the cytotoxicity of 9-nitropaullone (alsterpaullone) is not primarily due to CDK inhibition but an activation of caspase-8 and -9 through changes of the mitochondrial membrane potential, leading to apoptosis.[9]

Being involved in the development of metal-based antitumor drugs and, in particular, those of gallium,[10] we anticipated that the methyl thioimidate **2** (Scheme 1) will react with hydrazine to give novel species that can be further easily converted into paullones containing peripheral binding sites able to accommodate metal ions, and especially those of gallium. This approach was encouraged by our previous experience with the coordination of gallium to biologically active α-N-heterocyclic thiosemicarbazone.[11] Generally, coordinated gallium may endow tumor-inhibiting organic ligands with pharmacologically advantageous properties in a dual manner: first, because of the changed pharmacokinetics and the affinity of gallium to tumor cells and, second, because of its antiproliferative effects.[12−15] Experimental evidence shows that the critical target of the trivalent gallium cation is the iron-dependent enzyme ribonucleotide reductase,[16−18] but antimitotic effects[19] and interference with the mitochondrial membrane potential[20,21] may also be of pharmacological relevance. In view of the above-mentioned influence of paullones on the mitochondrial membrane potential, this metal is of special interest because it may contribute to the biological activity in a cooperative manner.

Herein we report on the synthesis of the first metal-based paullone derivative $[GaL_2]Cl$ and its X-ray diffraction structure, solid-state ^{13}C cross-polarization magic-angle spinning (CP MAS) NMR spectra, and cytotoxic activity in human cancer cell lines in vitro, which are compared to those of the metal-free ligand (HL) and compound **3** (see Scheme 1).

(6) Kunick, C.; Schultz, C.; Lemcke, T.; Zaharevitz, D. W.; Gussio, R.; Jalluri, R. K.; Sausville, E. A.; Leost, M.; Meijer, L. *Bioorg. Med. Chem. Lett.* **2000**, *10*, 567−569.

(7) Leost, M.; Schultz, C.; Link, A.; Wu, Y. Z.; Biernat, J.; Mandelkow, E. M.; Bibb, J. A.; Snyder, G. L.; Greengard, P.; Zaharewitz, D. W.; Gussio, R.; Senderowicz, A. M.; Sausville, E. A.; Kunick, C.; Meijer, L. *Eur. J. Biochem.* **2000**, *267*, 5983−5994.

(8) Knockaert, M.; Wieking, K.; Schmitt, S.; Leost, M.; Grant, K. M.; Mottram, J. C.; Kunick, C.; Meijer, L. *J. Biol. Chem.* **2002**, *277*, 25493−25501.

(9) Lahusen, T.; De Siervi, A.; Kunick, C.; Senderowicz, A. M. *Mol. Carcinog.* **2003**, *36*, 183−194.

(10) Galanski, M.; Arion, V. B.; Jakupec, M. A.; Keppler, B. K. *Curr. Pharm. Des.* **2003**, *9*, 2078−2089.

(11) Arion, V. B.; Jakupec, M. A.; Galanski, M.; Unfried, P.; Keppler, B. K. *J. Inorg. Biochem.* **2002**, *91*, 298−305.

(12) Bernstein, L. R. *Pharmacol. Rev.* **1998**, *50*, 665−682.

(13) Collery, P.; Keppler, B.; Madoulet, C.; Desoize, B. *Crit. Rev. Oncol. Hematol.* **2002**, *42*, 283−296.

(14) Jakupec, M. A.; Keppler, B. K. Metal Complexes in Tumor Diagnosis and as Anticancer Agents. In *Metal Complexes in Biological Systems*; Sigel, A., Sigel, H., Eds.; Marcel Dekker: New York, 2004; Vol. 42, pp 425−462.

(15) Jakupec, M. A.; Keppler, B. K. *Curr. Top. Med. Chem.* **2004**, *4*, 1575−1583.

(16) Chitambar, C. R.; Matthaeus, W. G.; Antholine, W. E.; Graff, K.; O'Brien, W. J. *Blood* **1988**, *72*, 1930−1936.

(17) Chitambar, C. R.; Narasimhan, J.; Guy, J.; Sem, D. S.; O'Brien, W. J. *Cancer Res.* **1991**, *51*, 6199−6201.

(18) Narasimhan, J.; Antholine, W. E.; Chitambar, C. R. *Biochem. Pharmacol.* **1992**, *44*, 2403−2408.

(19) Perchellet, E. M.; Ladesich, J. B.; Collery, P.; Perchellet, J. P. *Anti-Cancer Drugs* **1999**, *10*, 477−488.

(20) Zhang, D. W.; Colombini, M. *Biochim. Biophys. Acta* **1989**, *991*, 68−78.

(21) Gogvadze, V.; Zhukova, A.; Ivanov, A.; Khassanova, L.; Collery, P. In *Metal Ions in Biology and Medicine*; Collery, P., Corbella, J., Domingo, J. L., Etienne, J. C., Llobet, J. M., Eds.; John Libbey Eurotext: Paris, 1996; Vol. 4, pp 249−252.

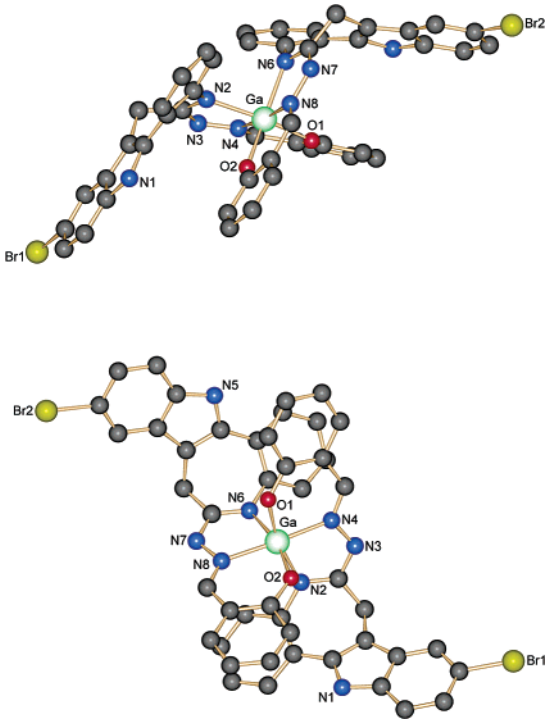

Figure 1. Views of the structure of $[GaL_2]^+$ parallel (top) and perpendicular (bottom) to one of the three-ring faces. Hydrogen atoms were omitted for clarity. Selected bond lengths (Å) and angles (deg): Ga−O1 1.901(2), Ga−O2 1.922(2), Ga−N2 2.101(2), Ga−N4 2.038(2), Ga−N6 2.121(2), Ga−N8 2.038(2); O1−Ga−N2 165.84(9), O2−Ga−N6 165.29(9), N4−Ga−N8 174.18(9).

Results and Discussion

Reaction of **2** with hydrazine hydrate in a 1:1 molar ratio in methanol afforded **3** in 36% yield after 48 h. The nucleophilic substitution of methanethiol in **2** for hydrazine takes place as shown in Scheme 1.

A condensation reaction of **3** with 2-hydroxybenzaldehyde in a 1:1 molar ratio in methanol produced **4** [which exists in solution as a mixture of two tautomers: the first (ca. 90%) with an exocyclic $C^6{=}N^{13}$ bond and the second (ca. 10%) with an endocyclic $C^6{=}N^5$ bond] in 93% yield (see the Experimental Section). The same reaction in the presence of 0.5 mol equiv of $GaCl_3$ and 1.0 mol equiv of NEt_3 resulted in the formation of $[GaL_2]Cl{\cdot}2.5H_2O$ (**5**·$2.5H_2O$) as a bright yellow complex with absorbance features at λ_{max} (ϵ_M, M^{-1} cm^{-1}) = 233 nm (90 250), 316 nm (53 152), and 399 nm (24 060) in methanol. The compound was stable in this solvent for at least 18 h (Figure S1 of the Supporting Information). The formation of the $[GaL_2]^+$ complex is confirmed by an electrospray ionization (ESI, positive) mass spectrum (MS), in which a 100% intense peak with *m*/*z* 959 is observed. The identity of this complex was also proved in the solid state by an X-ray diffraction study, the result of which is shown in Figure 1. $[GaL_2]Cl{\cdot}3CH_3OH$ (**5**·$3CH_3$-OH) crystallized from absolute methanol in the monoclinic space group $P2_1/c$ with one independent $[GaL_2]^+$ cation, one chloride anion, and three methanol molecules per asymmetric unit. Figure 1 illustrates the structure of the complex cation, with selected metrical parameters listed in the legend.

The gallium atom is coordinated by the two tridentate ligands in a meridional fashion. The coordination polyhedron approaches an octahedron with the configuration index *OC*-6-31,[22] where the two ligands are bound to the gallium atom through the phenolic oxygen atom, one of the hydrazine nitrogen atoms, and the nitrogen atom of the seven-membered azepine ring. The maximal deviation from linearity of the opposite atoms linked to gallium is about 15° (see the legend to Figure 1). The nitrogen seven-membered azepine ring atoms N2 and N6 of two L^- are located in cis positions. The angle between the two planes through GaO1N4N2 and GaO2N8N6 is 86.9°. A salient structural feature is the folded conformation of ligands bound to gallium. The bond lengths of the gallium atom to the nitrogen atoms are markedly longer compared to those to the oxygen atoms. The ligand backbone mainly consists of sp^2-hybridized carbon and nitrogen atoms. The only exception is the methylene group carbon atom in the seven-membered azepine ring, which is sp^3-hybridized. This atom interrupts the conjugation of the whole π system, and the ligand as a whole is nonplanar. In HL, restricted rotation around the phenyl−pyrrole axis (C12a−C12b in Scheme 1) enables ring inversion. The angles between the indolyl- and 2-hydroxybenzaldehyde moieties for both ligands are ca. 110° (110.4 and 110.8°), compared to 117.2° in the computed gas-phase structure of HL, using the *Gaussian 03* program package.[23] The hydroxybenzaldehyde moiety of one ligand is almost parallel with the six-membered benzazepine ring of the second ligand, possibly because of $\pi-\pi$ interaction between them.

The solid-state ^{13}C CP MAS NMR spectrum of **5**·$2.5H_2O$ is shown in Figure S2a of the Supporting Information. The number of resonance lines and their relative intensities are in agreement with the presence of 46 carbon atoms in the GaL_2^+ cation. While most signals appear in the spectrum as unresolved resonance lines, the presence of two well-resolved signals at 167.4 and 166.2 ppm, assigned to C17 in the first ligand and C17′ in the second one, is indicative of C_1 molecular symmetry of the $[GaL_2]^+$ cation. In addition to the above-mentioned two resonances (attributed to C17 and C17′), the nonquaternary suppression spectrum (Figure S2b of the Supporting Information) revealed four well-resolved signals at 127.7, 127.1, 125.4, and 124.9 ppm, which were

(22) Leigh, G., Ed. *IUPAC Nomenclature of Inorganic Chemistry. Recommendations*; Blackwell: Oxford, U.K., 1990; p 180.
(23) Frisch, M. J.; Trucks, G. W.; Schlegel, H. B.; Scuseria, G. E.; Robb, M. A.; Cheeseman, J. R.; Montgomery, J. A.; Vreven, T.; Kudin, K. N.; Burant, J. C.; Millam, J. M.; Iyengar, S. S.; Tomasi, J.; Barone, V.; Mennucci, B.; Cossi, M.; Scalmani, G.; Rega, N.; Petersson, G. A.; Nakatsuji, H.; Hada, M.; Ehara, M.; Toyota, K.; Fukuda, R.; Hasegawa, J.; Ishida, M.; Nakajima, T.; Honda, Y.; Kitao, O.; Nakai, H.; Klene, M.; Li, X.; Knox, J. E.; Hratchian, H. P.; Cross, J. B.; Adamo, C.; Jaramillo, J.; Gomperts, R.; Stratmann, R. E.; Yazyev, O.; Austin, A. J.; Cammi, R.; Pomelli, C.; Ochterski, J. W.; Ayala, P. Y.; Morokuma, K.; Voth, G. A.; Salvador, P.; Dannenberg, J. J.; Zakrewski, V. G.; Dapprich, S.; Daniels, A. D.; Strain, M. C.; Farkas, O.; Malick, D. K.; Rabuck, A. D.; Raghavachari, K.; Foresman, J. B.; Ortiz, J. V.; Cui, Q.; Baboul, A. G.; Clifford, S.; Cioslowski, J.; Stefanov, B. B.; Liu, G.; Liashenko, A.; Piskorz, P.; Komaromi, I.; Martin, R. L.; Fox, D. J.; Keith, T.; Al-Laham, M. A.; Peng, C. Y.; Nanayakkara, A.; Challacombe, M.; Gill, P. M. W.; Johnson, B.; Chen, W.; Wong, M. W.; Gonzalez, C.; Pople, J. A. *Gaussian 03*, revision B.04; Gaussian, Inc.: Pittsburgh, PA, 2003.

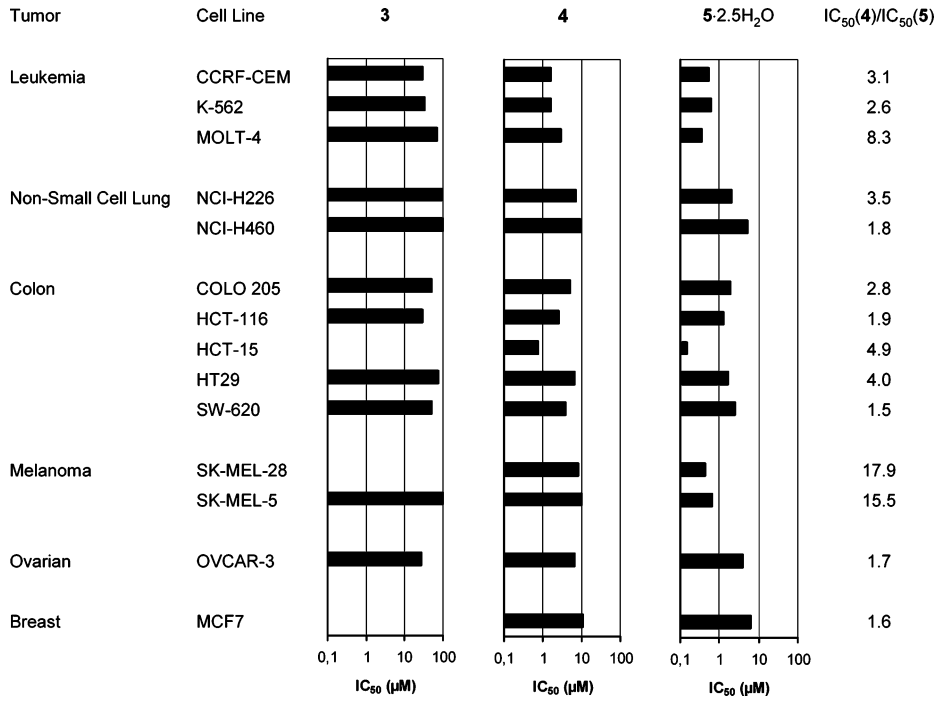

Figure 2. Cytotoxicity of **3**, **4**, and **5**·2.5H_2O in a panel of human tumor cell lines. IC_{50} values were interpolated from concentration−effect curves obtained by the XTT assay using a 48-h exposure. The ratios of the IC_{50} values of the uncomplexed paullone derivative **4** and its gallium complex **5**·2.5H_2O indicate the higher potency of the latter.

assigned to C7b, C7b′, C12b, and C12b′, respectively. This spectral pattern is also conclusive with the C_1 molecular symmetry of the cation in the solid-state structure of **5**·2.5H_2O. The number of resonance signals and their relative intensities are indicative of the presence of 20 quaternary carbon atoms in $[GaL_2]^+$. Furthermore, the difference spectrum in Figure S2c of the Supporting Information is in good agreement with the presence of 24 C−H groups in the same complex cation, giving strong evidence for the individuality of this gallium complex.

Compounds **3**−**5** were evaluated for their cytotoxicity in a panel of human tumor cell lines by means of a colorimetric microculture assay (XTT assay). IC_{50} values are depicted in Figure 2. The activity profiles of **3** and **4** resemble each other, but while the hydrazone **3** exerts only moderate cytotoxic effects, its condensation product with 2-hydroxybenzaldehyde (**4**) is roughly 1 order of magnitude more cytotoxic to all tumor cell lines employed, with IC_{50} values being in the 10^{-5}−10^{-6} M range. Even more remarkably, the gallium complex **5**·2.5H_2O is more cytotoxic than the uncomplexed paullone derivative **4** to all cell lines. As shown by the ratio IC_{50}(**4**)/IC_{50}(**5**·2.5H_2O) in Figure 2, the complex **5**·2.5H_2O is endowed with a 1.5−18-fold (on average 5.1-fold) higher cytotoxic potency than the ligand **4** alone. Thus, in contrast to findings with the iron chelator pyridoxal isonicotinoyl hydrazone published by Chitambar et al.[24,25] and our previous experience with an α-N-heterocyclic thiosemicarbazone,[11] coordination of gallium results in a much higher potency than could be explained by a simple stoichiometric effect, i.e., considering that one complex ion contains two coordinated ligand molecules. A comparison with data from the NCI (Bethesda, MD) suggests that the cytotoxicity of compound **5**·2.5H_2O also largely exceeds that of kenpaullone in most cell lines common to both panels because the reported GI_{50} values of kenpaullone range between 10^{-4} and 10^{-6} M.[26]

At first sight, the relative sensitivity patterns of the cell lines to compounds **4** and **5**·2.5H_2O appear to closely resemble each other. However, a noteworthy difference becoming obvious from Figure 2 is the overproportionally high sensitivity of the two melanoma cell lines to the gallium complex **5**·2.5H_2O (15.5 and 17.9-fold as compared to the uncomplexed paullone derivative **4** in SK-MEL-5 and SK-MEL-28 cells, respectively). Whether this difference reflects an improved uptake by these cells or qualitatively altered pharmacodynamic properties resulting from the coordination to gallium is as yet unclear.

Furthermore, it remains to be clarified whether the effect of the complex involves its dissociation into the cation and ligands and independent action of the components or whether the complex is endowed with a unique mode of action not attributable to the separate constituents. Because the parent compound **2** is a poor CDK1/cyclin B inhibitor, while exerting marked antiproliferative effects,[4] and because the increased steric demand of **4** and especially the gallium complex **5**·2.5H_2O is hardly compatible with the adenosine triphosphate binding pockets of CDKs, CDKs are rather unlikely to be the critical targets. Though speculative from the present state of knowledge, it is conceivable that the paullone derivative and gallium act in a cooperative manner

(24) Chitambar, C. R.; Boon, P.; Wereley, J. P. *Clin. Cancer Res.* **1996**, *2*, 1009−1015.
(25) Knorr, G. M.; Chitambar, C. R. *Anticancer Res.* **1998**, *18*, 1733−1738.
(26) http://dtp.nci.nih.gov/docs/dtp_search.html.

to perturb the mitochondrial membrane potential, as stated above. Future studies will have to address this question.

In conclusion, the reported results establish synthetic access to a new class of metal-based antiproliferative agents. The first gallium complex of a paullone derivative has been prepared and characterized by X-ray diffraction methods and solid-state ^{13}C CP MAS NMR spectroscopy. High antiproliferative activity in vitro of paullones is preserved when derivatization of the lactam unit to **3** and/or **4** is performed. Metalation of the derivatized paullones leads to a remarkable enhancement of the antiproliferative activity when compared to the metal-free paullone. The chemistry reported will be further explored for the preparation of species with 1:1 and 1:2 metal-to-ligand stoichiometries.

Experimental Section

Starting Materials. 9-Bromo-6-(methylthio)-7,12-dihydroindolo-[3,2-*d*][1]benzazepine (**2**) was prepared as described by Kunick et al.[4] Gallium chloride, hydrazine hydrate, triethylamine, and 2-hydroxybenzaldehyde were purchased from Aldrich and used as received.

9-Bromo-7,12-dihydroindolo[3,2-*d*][1]benzazepin-6-ylhydrazine (3). To a suspension of **2** (0.71 g, 2.0 mmol) in dry ethanol (50 mL) was added hydrazine hydrate (0.2 mL). After 2 days, the precipitate formed was filtered off, washed with ethanol, and dried in air. Yield: 0.24 g, 35.8%. Anal. Calcd for $C_{16}H_{13}N_4Br$ (%): C, 56.32; H, 3.84; N, 16.42. Found: C, 56.19; H, 3.80; N, 16.22. ESI-MS (negative) *m*/*z* (rel intens, %): 340 (100) [**3** − H]$^-$. IR spectrum in KBr, selected bands, cm^{-1}: 1645, 1467, 1308, 752. UV−vis (methanol) λ_{max}, nm (ϵ, M^{-1} cm^{-1}): 231 (50 350), 319 (21 990). ^1H NMR δ_H (400.13 MHz, DMSO-d_6): 3.40 (s, 2H, C^7H_2), 3.8−6.6 (vbs, 3H, $NHNH_2$), 7.09 (dd, $^3J_{HH}$ = 8.0 and 7.5 Hz, 1H, C^2H), 7.23 (d, $^3J_{HH}$ = 8.5 Hz, 1H, $C^{10}H$), 7.27 (d, $^3J_{HH}$ = 8.0 Hz, 1H, C^4H), 7.29 (dd, $^3J_{HH}$ = 7.5 and 8.0 Hz, 1H, C^3H), 7.36 (d, $^3J_{HH}$ = 8.5 Hz, 1H, $C^{11}H$), 7.65 (d, $^3J_{HH}$ = 8.0 Hz, 1H, C^1H), 7.76 (s, 1H, C^8H), 11.63 (s, 1H, $N^{12}H$). ^{13}C NMR δ_C (100.63 MHz, DMSO-d_6): 28.0 (C^7), 112.2 (C^9), 114.1 (C^{11}), 120.8 (C^8), 121.9 (C^2 and C^4), 124.8 (C^{10}), 128.0 (C^1), 128.9 (C^3), 129.1 (C^{12a}), 136.5 (C^{11a}). For atom labeling, see Scheme 1.

***N*-(9-Bromo-7,12-dihydroindolo[3,2-*d*][1]benzazepin-6(5*H*)-yliden-*N*′-(2-hydroxybenzyliden)azine, HL (4).** To **3** (0.12 g, 0.35 mmol) in boiling methanol (30 mL) was added 2-hydroxybenzaldehyde (0.04 g, 0.35 mmol), and the suspension was heated until all starting material had dissolved. The next day the precipitate formed was filtered off, washed with methanol, and dried in air. Yield: 0.15 g, 92.5%. Anal. Calcd for $C_{23}H_{17}N_4BrO$ (%): C, 62.04; H, 3.85; N, 12.58. Found: C, 61.69; H, 3.67; N, 12.44. ESI-MS (negative) *m*/*z* (rel intens, %): 445 (100) [**4** − H]$^-$. IR spectrum in KBr, selected bands, cm^{-1}: 3415, 1626, 1465, 744. UV−vis (methanol) λ_{max}, nm (ϵ, M^{-1} cm^{-1}): 229 (48 850), 319 (24 810).

Tautomer with an Exocyclic Double C=N Bond. ^1H NMR δ_H (400.13 MHz, DMSO-d_6): 3.66 (s, 2H, C^7H_2), 6.88 (m, 1H, $C^{20}H$), 6.89 (m, 1H, $C^{18}H$), 7.26 (m, 1H, C^2H), 7.27 (m, 1H, $C^{19}H$), 7.28 [m, 1H, $C^{10}H$], 7.38 [m, 1H, C^3H], 7.40 [m, 1H, $C^{11}H$], 7.56 [m, 1H, C^4H], 7.71 (m, 1H, $C^{21}H$), 7.73 (m, 1H, C^1H), 7.90 (s, 1H, C^8H), 8.61 (s, 1H, $C^{15}H$), 9.23 (s, 1H, N^5H), 10.62 (s, 1H, $C^{17}OH$), 11.82 (s, 1H, $N^{12}H$). ^{13}C NMR δ_C (100.63 MHz, DMSO-d_6): 28.3 (C^7), 110.1 (C^{7a}), 112.6 (C^9), 114.3 (C^{11}), 116.9 (C^{18}), 120.0 (C^{20}), 120.6 (C^{16}), 121.2 (C^8), 122.9 (C^{12b}), 123.8 (C^4), 124.0 (C^2), 125.3 (C^{10}), 128.1 (C^1), 129.1 (C^{7b}), 129.1 (C^3), 131.0 (C^{21}), 132.2 (C^{19}), 135.2 (C^{12a}), 136.8 (C^{11a}), 137.7 (C^{4a}), 155.8 (C^{15}), 157.7 (C^6), 158.3 (C^{17}). For atom labeling, see Scheme 1.

Tautomer with an Endocyclic Double C=N Bond. ^1H NMR δ_H (400.13 MHz, DMSO-d_6): 4.01 (s, 2H, C^7H_2), 6.96 (m, 1H, $C^{20}H$), 7.04 [m, 1H, $C^{18}H$], 7.25 [m, 1H, $C^{10}H$], 7.33 [m, 1H, $C^{19}H$], 7.58 (m, 1H, C^4H), 8.55 (s, 1H, $C^{15}H$), 10.08 (s, 1H, $N^{13}H$), 11.84 (s, 1H, $N^{12}H$). ^{13}C NMR δ_C (100.63 MHz, DMSO-d_6): 21.5 (C^7), 108.2 (C^q), 112.7 (C^q), 114.5 (CH), 116.7 (C^{18}), 120.2 (C^{20}), 120.3 (C^q), 120.7 (CH), 122.4 (C^q), 123.6 (CH), 123.7 (C^{10}), 128.0 (CH), 128.8 (C^q), 129.4 (CH), 130.8 (CH), 131.3 (C^4), 131.8 (C^{19}), 136.2 (C^q), 136.9 (C^q), 155.0 (C^{15}), 158.4 (C^q), 158.9 (C^q), 165.1 (C^q). Seven superimposed proton signals (shown in square brackets) could not be unequivocally assigned.

[GaL_2]Cl·2.5H_2O (5·2.5H_2O). To a boiling solution of **3** (0.17 g, 0.49 mmol) in methanol (30 mL) was added 2-hydroxybenzaldehyde (0.06 g, 0.49 mmol) in methanol (1 mL). The reaction mixture was refluxed until the starting material had dissolved and the Schiff base **4** started to crystallize (ca. 15 min). At this point, a solution of $GaCl_3$ (0.25 mmol) in ethanol (0.3 mL) was added. The solution was refluxed for 20 min and allowed to cool to room temperature. The precipitate formed was filtered off the next day, washed with cold methanol, and dried in vacuo. Yield: 0.09 g, 35%. The yield can be increased up to 0.14 g (55%) if the reaction is carried out in the presence of Et_3N (0.05 g, 0.5 mmol). Anal. Calcd for $C_{46}H_{37}N_8Br_2ClGaO_{4.5}$ (%): C, 53.19; H, 3.59; N, 10.79. Found: C, 53.05; H, 3.63; N, 10.39. ESI-MS (positive) *m*/*z* (rel intens, %): 959 (100) [GaL_2]$^+$. IR spectrum in KBr, selected bands, cm^{-1}: 1581, 1389, 1304. UV−vis (methanol) λ_{max}, nm (ϵ, M^{-1} cm^{-1}): 233 (90 250), 316 (53 152), 399 (24 060). ^{13}C NMR δ_C (75.47 MHz, CP MAS): 25.2 (C^7, $C^{7\prime}$), 108.1 (C^{7a}, $C^{7a\prime}$, C^9 or C^{7a}, C^9, $C^{9\prime}$), 115.3 (C^{16}, $C^{16\prime}$, $C^{9\prime}$ or C^{7a}), 115.6, 114.8, 112.2 (C^{11}, $C^{11\prime}$, C^{18}, $C^{18\prime}$), 120.3 (C^8, $C^{8\prime}$, C^{20}, $C^{20\prime}$), 127.2, 125.7 (C^1, $C^{1\prime}$, C^2, $C^{2\prime}$, C^3, $C^{3\prime}$, C^4, $C^{4\prime}$, C^{10}, $C^{10\prime}$), 127.7, 127.1, 125.4, 124.9 (C^{7b}, $C^{7b\prime}$, C^{12b}, $C^{12b\prime}$), 134.6, 133.4 (C^{19}, $C^{19\prime}$, C^{21}, $C^{21\prime}$), 139.1, 137,9, 136.4, 134.5 (C^{4a}, $C^{4a\prime}$, C^{11a}, $C^{11a\prime}$, C^{12a}, $C^{12a\prime}$), 151.3 (C^6, $C^{6\prime}$), 152.9 (C^{15}, $C^{15\prime}$), 167.4 (C^{17} or $C^{17\prime}$), 166.2 (C^{17} or $C^{17\prime}$). For atom labeling, see Scheme 1. Solution ^{13}C NMR spectra were not measured because of solubility problems.

X-ray Crystallography. Details of data collection procedures and structure refinement for **5**·3CH_3OH are given in the Supporting Information. A single crystal of suitable size was attached to a glass fiber using acrylic resin and mounted on a goniometer head at 30 mm from the detector. Data were collected on a Nonius Kappa CCD diffractometer using graphite-monochromated X radiation (λ = 0.710 73 Å) at 120 K. A total of 455 frames were measured, each for 55 s over a 1.5° scan width. The data were processed using Denzo-SMN software.[27] The structure was solved by direct methods and refined by full-matrix least-squares techniques. Non-hydrogen atoms were refined with anisotropic displacement parameters. Hydrogen atoms were inserted at calculated positions and refined with a riding model. The following computer programs were used: structure solution, *SHELXS-97*;[28] refinement, *SHELXL-97*;[29] molecular diagrams, *Schakal-97*;[30] computer, Pentium IV; scattering factors.[31]

NMR Spectroscopy, ESI Mass Spectrometry, und UV−Vis Spectroscopy. ^1H, $^{13}C\{^1H\}$, $^1H-^1H$ COSY, and $^{13}C-^1H$ COSY

(27) Otwinowski, Z.; Minor, W. *Macromol. Crystallogr., Part A* **1997**, 307−326.
(28) Sheldrick, G. M. *SHELXS-97, Program for Crystal Structure Solution*; University of Göttingen: Göttingen, Germany, 1997.
(29) Sheldrick, G. M. *SHELXL-97, Program for Crystal Structure Refinement*; University of Göttingen: Göttingen, Germany, 1997.
(30) Keller, E. *Schakal-97*; Kristallographisches Institut, Universitaet Freiburg: Freiburg, Germany, 1997.
(31) *International Tables for X-ray Crystallography*; Kluwer Academic Press: Dordrecht, The Netherlands, 1992; Vol. C, Tables 4.2.6.8 and 6.1.1.4.

spectra were recorded in DMSO-d_6 at 298 K (2D in a gradient-enhanced mode) using a Bruker Avance DPX 400 instrument (UltraShield Magnet) and standard pulse programs at 400.13 (^{1}H) and 100.62 MHz (^{13}C). Chemical shifts were measured relative to the solvent peak. Solid-state ^{13}C CP MAS NMR spectra were measured on a Bruker MSL-300 spectrometer equipped with a CP MAS double-bearing probe and a Bruker BV-1000 temperature control unit. The ZrO_2 rotor (7-mm internal diameter) was charged with the complex and sealed by a Kel-F insert. The optimal contact time for ^{13}C CP was 2−3 ms. The spinning rate was 4.33 kHz. The external standard was adamantane [$\delta(CH_2) = 38.40$ relative to tetramethylsilane]. ESI mass spectrometry was carried out with a Bruker Esquire 3000 instrument (Bruker Daltonic, Bremen, Germany). The given *m*/*z* values, originating from the most intense isotopes, were obtained by the mass linearization procedure. Expected and experimental isotope distributions were compared. UV−vis spectra were recorded on a Perkin-Elmer Lambda 20 UV−vis spectrophotometer using samples dissolved in methanol.

Computational Details. Ab initio computations were performed using the *Gaussian 03* program package.[23] Gas-phase calculations were carried out using density functional theory (DFT) with Becke's three-parameter hybrid functional[32] using the correlation functional of Lee, Yang, and Parr (B3LYP).[33,34] The 6-31G* basis set was used for carbon, nitrogen, oxygen, and hydrogen atoms. Three sets of d polarization functions and one set of f functions in addition were used for the bromine atom [6-31G(3df)]. The performed vibrational analysis showed that the gas-phase structure reported for **4** is the minimum (NIMAG = 0) on the potential energy surfaces. Starting coordinates for **4** were available from an X-ray diffraction study of **5**·3CH_3OH.

Cell Lines and Culture Conditions. Human leukemia (CCRF-CEM, K-562, and MOLT-4), nonsmall cell lung cancer (NCI-H460 and NCI-H226), colon cancer (COLO 205, HCT-116, HCT-15, HT29, and SW-620), melanoma (SK-MEL-28 and SK-MEL-5), ovarian cancer (OVCAR-3), and breast cancer (MCF7) cell lines were obtained from the American Type Culture Collection and propagated in an appropriate cell culture medium (RPMI 1640 or DMEM) supplemented with 10% heat-inactivated fetal calf serum. Cultures were maintained at 37 °C in a humidified atmosphere containing 5% CO_2.

Cytotoxicity Assay. The cytotoxicities of the test compounds were determined by means of a colorimetric assay {XTT assay, where XTT = 2,3-bis(2-methoxy-4-nitro-5-sulfophenyl)-5-[(phenylamino)carbonyl]-2*H*-tetrazolium hydroxide}. Briefly, cells were harvested from culture flasks (by trypsinization in the case of adherent cell lines), seeded in a 100-μL cell culture medium in defined densities (ranging from 5×10^3 to 4×10^4 vital cells per well, depending on the cell line) into 96-well microculture plates, and incubated at 37 °C for 24 h. Stock solutions of the test compounds in dimethyl sulfoxide (DMSO; 5 mM) were sterilized by filtration (0.2 μm) and serially diluted in a cell culture medium such that the effective DMSO content did not exceed 2%. A total of 100 μL of each dilution was added to the cells in triplicate. Negative control microcultures received a 100-μL drug-free cell culture medium, while positive controls were deadened with phenol. After drug exposure for 48 h at 37 °C, a 40-μL XTT (Sigma-Aldrich) solution (1 mg/mL of phosphate-buffered saline) was added to each well, and cells were incubated with XTT for 8 h at 37 °C. The formazan developed in the presence of vital cells was quantified in a microplate reader (Genios, Tecan) at 450 nm using a reference wavelength of 690 nm. The raw data were normalized to the positive control and set in relation to the metabolic activity of the negative control. IC_{50} values were calculated from concentration−effect curves by four-parametric nonlinear regression using Graph Pad Prism 3.0 software.

Acknowledgment. This research was supported by FWF (Austrian Science Fund). Support and sponsorship by COST Action D20 is kindly acknowledged. The authors thank Prof. Dr. G. Giester for X-ray data collection and Ion Chiorescu for geometry optimization of HL (**4**) by DFT calculations.

Supporting Information Available: UV−vis and solid-state ^{13}C CP MAS NMR spectra of **5**·2.5H_2O, details of X-ray data collection and refinement, and additional structural data for [GaL_2]Cl·3CH_3OH (CIF). This material is available free of charge via the Internet at http://pubs.acs.org.

IC0511120

(32) Becke, A. D. *J. Chem. Phys.* **1993**, *98*, 5648−5652.
(33) Lee, C.; Yang, W.; Parr, R. G. *Phys. Rev. B* **1988**, *37*, 785−789.
(34) Miehlich, B.; Stoll, H.; Preuss, H. *Chem. Phys. Lett.* **1989**, *157*, 200−206.